

Case study

An improved solution of local window parameters setting for local singularity analysis based on Excel VBA batch processing technology



Daojun Zhang^a, Qiuming Cheng^{b,c,*}, Frits Agterberg^d, Zhijun Chen^e

^a College of Economics and Management, Northwest A&F University, Yangling 712100, PR China

^b State Key Laboratory of Geological Processes and Mineral Resources, China University of Geosciences, Wuhan 430074, PR China

^c Department of Earth and Space Science and Engineering, York University, Toronto, Canada M3J1P3

^d Geological Survey of Canada, 601 Booth Street, Ottawa, ON, Canada K1A0E8

^e Faculty of Earth Resources, China University of Geosciences, Wuhan 430043, PR China

ARTICLE INFO

Article history:

Received 10 February 2015

Received in revised form

30 November 2015

Accepted 14 December 2015

Available online 17 December 2015

Keywords:

Local singularity index mapping

Anisotropy

Multiple-scale

Optimization

MS-Excel

VBA

Mineral resource assessment

ABSTRACT

In this paper Excel VBA is used for batch calculation in Local Singularity Analysis (LSA), which is for the information extracting from different kinds of geoscience data. Capabilities and advantages of a new module called Batch Tool for Local Singularity Index Mapping (BTLSIM) are: (1) batch production of series of local singularity maps with different settings of local window size, shape and orientation parameters; (2) local parameter optimization based on statistical tests; and (3) provision of extra output layers describing how spatial changes induced by parameter optimization are related to spatial structure of the original input layers.

© 2015 Elsevier Ltd. All rights reserved.

1. Introduction

Separating anomalies from background according to an assumed threshold is essential both in exploration geochemistry and environmental geochemistry. Geochemical anomalies have been used as one of the most important ore guides of prospecting for many years, in which statistical methods play a great role (Harris et al., 1999, 2000). Classical statistical methods such as univariate and multivariate analysis methods based on frequency statistics and were popular over a long period in the past (e.g. Sinclair, 1974; Govett et al., 1975; Miesch, 1981; Stanley and Sinclair, 1989). However, due to the effects of soil and vegetation cover, geochemical signatures and geophysical features obtained at the surface of the Earth can be very weak since measured values obtained by geochemical analysis are mixed with both anomaly parts which reflect deep orebody and background parts which reflect soil background effect. Classical first-order and second-order statistics will be of limited use in this condition. Higher order statistics based on fractal/multiracial theory has been developed to

deal with this problem (Cheng, 2008). Fractal was originally used to characterize self-similarity of geometric objects at different scales: i.e., amplified parts are like the whole to some degree (Mandelbrot, 1975; Cheng et al., 1994). Cheng et al. (1994) and Cheng (1996) used this self-similarity for the description of cumulative frequency, and developed concentration–area (C–A) model, which was considered as the first attempt to use fractal method to separate geochemical anomalies from background (Li et al., 2003). In C–A model, an accumulative frequency distributing graph is obtained, in which the logs of concentration and the area which own values greater than corresponding concentration are taken as abscissa and ordinate respectively. One or more straight lines can be used to fit the accumulative frequency distributing, and their slopes represent different fractal dimensions (Cheng et al., 1994). C–A model incorporates spatial association, anisotropy information and locational information into characterization of geochemical patterns, however it is of limited use in the context of changing background. Later, Cheng (1997, 1999b, 2005) proposed local singularity analysis (LSA) technology which can be seen as an application of the C–A model within a local window for local anomaly information extraction (Cheng, 2006b). According to (Cheng, 2004, 2006a), abnormally strong energy release within a very short time interval or massive emplacement of material

* Corresponding author at: State Key Laboratory of Geological Processes and Mineral Resources, China University of Geosciences, Wuhan 430074, PR China.

E-mail address: qiuming@yorku.ca (Q. Cheng).

within a very small spatial domain can result in a singularity, and LSA is a technology to explore this singularity.

LSA, if implemented in spatial domain, is essentially a spatial neighborhood-window statistical model based on nonlinear theory with GIS-based applications. In this approach, fractal/multi-fractal theory is used to overcome limitations of classical statistical methods based on the assumption of normal or lognormal distribution of the data (Cheng, 1996). Application of the local window statistical method can avoid the problem that a global optimal threshold may not be suitable at every location as is generally assumed in traditional statistical methods. Because of this advantage, LSA has become widely used in the geosciences and has been established as a powerful tool for information extraction of geochemical (Cheng, 2007; Zuo & Cheng, 2008; Xie et al., 2008; Zuo et al., 2009, 2013, 2015; Liu et al., 2013a, 2013b), tectonic (Wang et al., 2012), geophysical (Wang et al., 2013; Chen et al., 2013, 2015), DEM (Zhang et al., 2014), remote sensing (Neta et al., 2010) and land-value assessment data (Hu et al., 2012). Nevertheless, none of these papers offer any case study considering anisotropy and its variability in space.

In fact, Cheng (2006a) pointed out that LSA can be implemented both based on regular windows of different shapes and contours of irregular shapes which characterize the anisotropy of geochemical patterns, and Cheng (1999a) once introduced rules for LSA application including how to build a moving window and how to set the window's parameters by using the spatial U-statistics method (Cheng et al., 1996). Chen (2007), Chen et al. (2007a, 2007b, 2014) proposed several algorithms to estimate implement LSA including an iterative approach (I-LSA) and a generalized approach accounting for anisotropies (GLSA). I-LSA produces a sequence of singularities (α) at various scales to be combined for estimation of singularity, and GLSA estimates singularity with windows in variable sizes and shapes as proposed and used by Cheng et al. (1996) for spatial U-statistics analysis. However, LSI based on U-statistics is very time-consuming because of its high complexity, and in fact very few applications have been performed based on it.

On the whole, it is not efficient to model LSA with existing software or modules, and it cannot always fit each location to use the same set of local window parameters. In this paper we develop a new program in VBA, the built-in programming language of Microsoft Office, for LSA with variable windows. Advantages of Excel VBA for LSA include: (1) it can directly call a large number of built-in Excel Functions which are efficient and easy to use (here the primary concerns are math and trig functions and statistical functions); (2) design automation of parts of the program can be achieved by the use of macro recording, which greatly benefits us the file reading and writing programming; and (3) Microsoft Office is the world's most widely used office software and modules developed in Excel VBA can be directly used by almost all Microsoft Windows users, which facilitates the application of LSA. For these reasons, Excel VBA was chosen in this paper associated with the secondary development environment of ArcGIS 10 to develop a comprehensive and virtualized module for LSA called Batch Tool for Local Singularity Index Mapping (BTLSIM). Following are the main features and advantages of this new module compared with present software tools.

(1) BTLSIM provides a batch processing for LSI. Supposing there are 40 chemical element layers, and we need to obtain their LSI layers at the local window size of 6 km, 8 km, ..., 50 km, then it needs $40 \times 23 = 920$ times' manual operations. If anisotropy is considered, and further supposing there are 9 kinds of directions and 10 kinds the length ratios between the semi-minor and semi-major axes of the elliptical window, manual operations needed to be done would be

$40 \times 23 \times 9 \times 10 = 82,800$ times, which not only costs lots of time, but increases the wrong making probability. One need not worry about these problems at all when BTLSIM is performed.

- (2) BTLSIM offers more window parameters, which are classified as calculation window and file window parameters, and users have more choices. E.g., if the study area is large and there are too many grids, one can increase the interval of calculation window size which can only be 1 in present software; local elliptical windows which are used to describe anisotropy can be defined arbitrarily by specifying the orientation of the ellipse's major axis, and the length ratio of major and minor axis, while we can only select four directions and the length ratio cannot be modified in existing software.
- (3) Based on the multi-scale and anisotropic window parameters introduced above, one can obtain many LSI layers together with their statistical test parameter layers reflecting the significance level of LSI at each location, which makes it possible to obtain an optimized LSI (OLSI) at each location together with its self-adaptive local window parameters (SALWP) including self-adaptive local window size (SALWS), self-adaptive local window direction (SALWD) and self-adaptive local window compression ratio (SALWCR). The case study in research shows that OLSI layer has better spatial relationship with known deposits than any single LSI layers, and SALWP can indicate more tectonic and metallogenic information in the study area.
- (4) Average value for a local window can be measured using not only the arithmetic mean, but also the median, which is considered as a robust statistic.

Although Excel VBA is used for BTLSIM programming in this paper, our research can provide references for people who use other programming tools and are interested in LSI algorithm improvement. More importantly, this research can benefit people who have already used LSI for geo-information extraction since BTLSIM simplifies operational processes and improves efficiency and prediction accuracy. Besides, the solutions provided in this study to deal with multi-scale and anisotropy, and the realization of anisotropic parameter mapping can also be referred by potential geosciences researchers.

2. Theory of local singularity analysis

The basic idea for LSA is to deduce a regression equation based on the logs of both window size and the concentration within it so obtain LSI from the slope of the equation, and before that the most important choice in LSA consists of the selection of an appropriate window size: too small window size captures more detailed information but can incorporate random noise, whereas too large window size results in relatively low resolution maps. LSI is obtained by means of the following power-law model in two-dimensional space:

$$\rho(\varepsilon) = c\varepsilon^{\alpha-2} \quad (1)$$

where c is a constant, representing a density measure that is independent of scale, ε is the local window size, ρ is average density within the local window of size ε , and α is the singularity index. By using the least squares method, α can be estimated as the slope of a best-fitting straight line for the relation between $\log \rho$ and $\log \varepsilon$. The local singularity index α has the following properties: (1) when α is close to 2, element concentration is substantially constant, regardless of window size; (2) $\alpha < 2$ represents concentration value increase for reduced window size, indicating

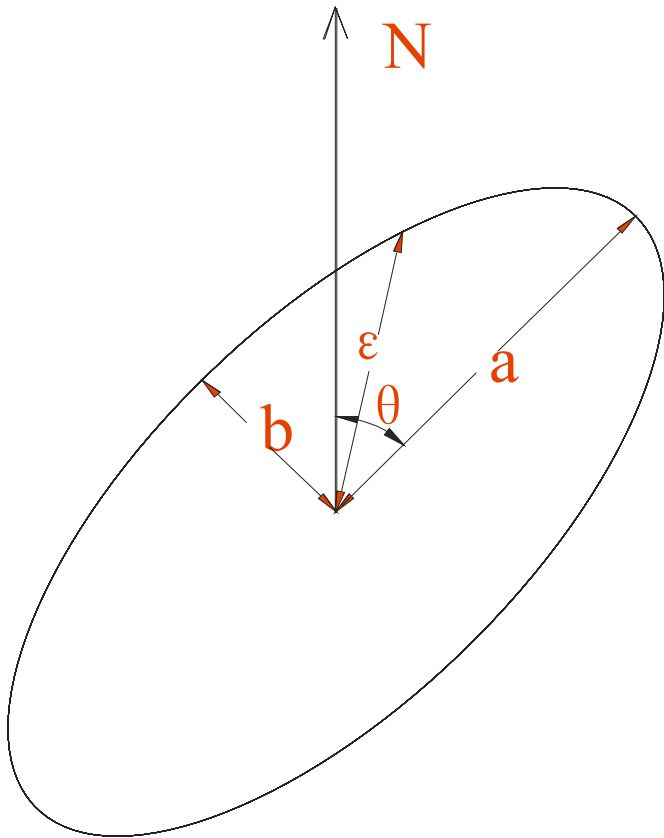


Fig. 1. Anisotropic parameters for elliptical window.

elliptical window with variable shape, orientation and size, it can be used for measuring anisotropic singularity as shown in Fig. 1 (Cheng, 1999a). For an elliptical window, Eq. (1) becomes

$$\rho(\varepsilon(a, \beta, \theta)) = c(a, \beta, \theta)\varepsilon^{\alpha-2}(a, \beta, \theta) \quad (2)$$

where ε is the equivalent radius with $\beta=b/a$ being the ratio of semi-minor axis (b) to semi-major axis (a) and θ representing azimuth. Equivalent radius is used for window characterization size rather than semi-major or semi-minor axis. The singularity index is obtained as the slope of the best-fitting line for the log-log relationship between window size $\varepsilon(a, \beta, \theta)$ and average content $\rho(\varepsilon(a, \beta, \theta))$. In this study, this kind of anisotropic window is also included in BTLSIM as an extension of isotropic window. Besides, a deeper contribution of BTLSIM is that it can obtain different anisotropic parameters for different locations, which is important to perform LSI in more complicated area, and to map anisotropic parameters for further information mining.

3. Models

Elliptical parameters are used to express anisotropy in BTLSIM. The main part of BTLSIM is implemented with Excel VBA, while other procedures are performed with ArcToolbox and Python in ArcGIS 10.0 Desktop. Fig. 2 shows the processing flow of BTLSIM taking geochemical exploration data for example.

*a, LSA is local singularity analysis; *b, LSI is local singularity index. The dotted rounded rectangle at the top contains all modules developed with ArcToolbox and Python in ArcGIS 10.0 Desktop; dotted rounded rectangle at the bottom contains the modules developed based on Excel VBA. The rounded rectangles colored in yellow are resulting maps to be shown in ArcGIS 10, while the ones colored in green are operational process documents produced by BTLSIM.

3.1. Data format transformation

Grid files must be transformed into ASCII files in order to perform BTLSIM, while the resulting ASCII files of BTLSIM have to be transformed into ArcGIS GRID in order to be shown in ArcGIS. Auxiliary tools have been developed with ArcToolbox and Python,

enrichment in the vicinity during the process of mineralization; and (3) when $\alpha > 2$, concentration decreases with the decrease of window size indicating depletion.

The window can be of different shape, e.g. square, circular or elliptical (Cheng, 1999a) and can incorporate even contours of natural shapes determined by the data (Cheng 2006a). For a regular window, it can be determined by the size ε representing length of side, radius, or equivalent radius, respectively. As an

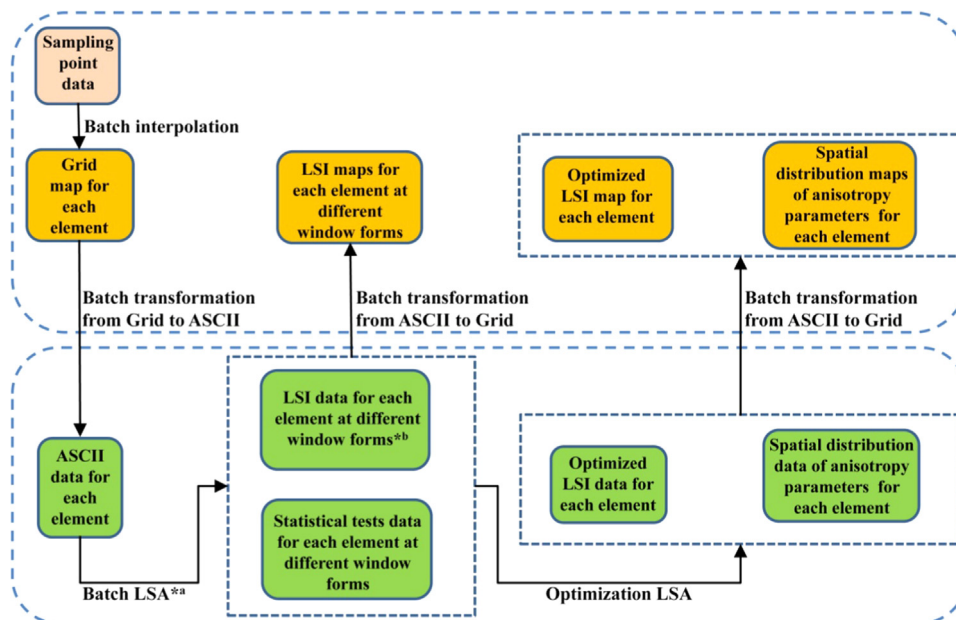
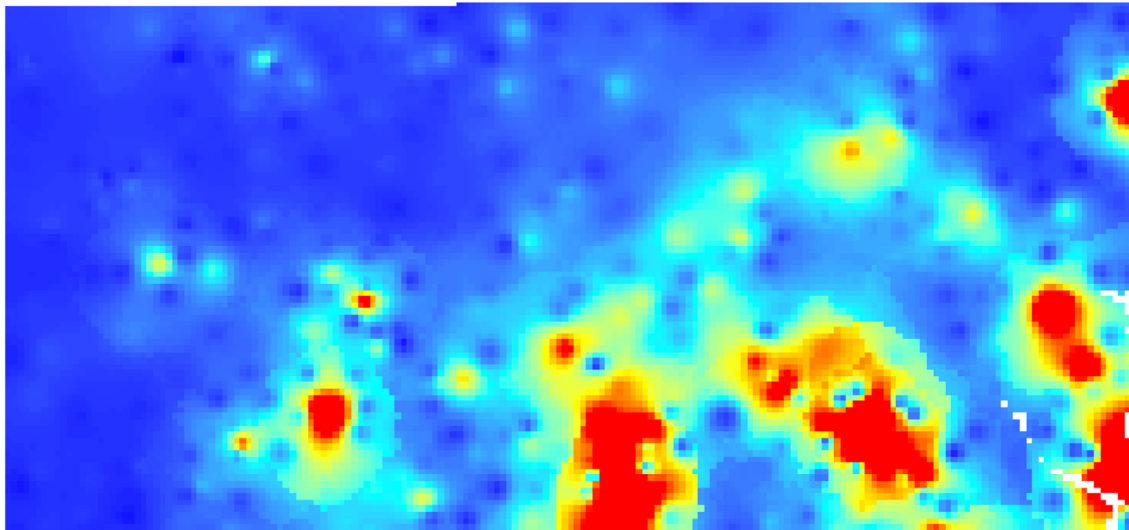


Fig. 2. Processing flow of Local Singularity Index Mapping.



(a) ArcGIS GRID

```

ncols           183
nrows           227
xllcorner       302869.799949
yllcorner       4832488.7674181
cellsize        500
NODATA_value    -9999
-9999 -9999 -9999 -9999 -9999 -9999 -9999 -9999 -9999 -9999 -9999 -9999 -9999 -9999 -9999 -9999 -9999 -9999 -9999 -9999
3 2.586167 2.520388 2.543285 2.686834 2.871292 3.152994 3.510174 3.976501 4.600021 5.40504 6.306086 7.007425 7.
3.264577 3.290315 3.317501 3.346402 3.320493 3.352246 3.391467 3.441835 3.507206 3.59128 4.107793 4.260533 4.42
.720981 2.715063 2.715357 2.712064 2.725328 2.713479 2.676635 2.697529 2.735846 2.783751 2.832067 2.873323 2.90
3.247118 3.275149 3.303924 3.332295 3.36222 3.342489 3.379276 3.428896 3.496683 3.588063 3.708364 4.271666 4.47
279 2.662559 2.666054 2.677845 2.677922 2.676714 2.64752 2.638371 2.639255 2.691802 2.756416 2.819371 2.873536
3.22838 3.261044 3.292708 3.320915 3.347013 3.331369 3.362991 3.409097 3.476454 3.572168 3.703945 3.880105 4.50
2.590795 2.614074 2.647715 2.650824 2.633387 2.579356 2.556361 2.578927 2.650561 2.733505 2.810199 2.87639 2.92
3.206643 3.2489 3.28699 3.315396 3.335014 3.354774 3.342819 3.382515 3.446217 3.542194 3.680217 3.87202 4.51027
2.524057 2.562067 2.621541 2.643774 2.611905 2.53727 2.502671 2.551145 2.653437 2.758886 2.806242 2.880222 2.94
3.178147 3.238655 3.291258 3.320137 3.327601 3.33198 3.350227 3.43011 3.406744 3.498352 3.635476 3.832065 4.106
02527 2.548031 2.620417 2.669504 2.634529 2.560457 2.527947 2.576644 2.672891 2.762974 2.800093 2.876683 2.9614
3.132561 3.229516 3.314239 3.342777 3.321068 3.299843 3.307717 3.376043 3.444667 3.54749 3.570914 3.759082 4.02
.59277 2.669737 2.707874 2.692083 2.64869 2.62644 2.664364 2.719113 2.75377 2.76688 2.848028 2.996875 3.074427
3.043701 3.212775 3.376351 3.401144 3.291512 3.229224 3.249941 3.29096 3.381589 3.472096 3.605399 3.792004 3.89
3501 2.759374 2.771704 2.711021 2.752209 2.741129 2.7412 2.724528 2.685009 2.693589 2.800441 2.986498 3.129539
2.862912 3.158756 3.521778 3.576851 3.126454 3.05284 3.181745 3.243902 3.317893 3.389716 3.503592 3.665571 3.87
78292 2.799396 2.855882 2.854793 2.859989 2.849542 2.828436 2.783112 2.689395 2.574846 2.560054 2.711956 2.9787
2.600141 3.03825 3.760943 4.327147 2.734806 2.918211 3.170784 3.208155 3.214301 3.29441 3.39036 3.531013 3.7009
4 2.963373 2.981364 2.956469 2.944536 2.909261 2.83153 2.691533 2.546116 2.522049 2.71068 3.052587 3.406194 3.7

```

(b) ASCII Code

Fig. 3. Data format transformation between (a) ArcGIS Grid and (b) ASCII, obtained through printscreen.

with which grid and ASCII can be transformed into each other in batches in accordance with a predetermined directory (Fig. 3).

3.2. Main module

In this study the main module design of BTLSIM is based on Excel VBA. Fig. 4 provides two user interfaces which show all parameters and how to set them in BTLSIM. One is for local singularity index batch calculation with isotropy or anisotropy parameters, and the other is for optimized window parameter selection.

3.2.1. Multiple-file design

A source folder should be created first, so that all ASCII files at a specific location can be read and saved individually into a nested two-dimensional array for further processing. Analogously, a result saving folder should be assigned, so that the resulting data can be saved successively as ASCII files from another nested array.

3.2.2. Multiple-local-window design

Please keep in mind that “window” in this paper means sliding local window, i.e., a range in which LSI is calculated for the current point (grid). This part involves two types of window: calculation windows within each of which the average content will be calculated, and file windows for each of which a LSI layer will be obtained. A circular window example is given in Fig. 5 for understanding their interrelationship. The point to be calculated for LSI value is called current point, which is located at the center in Fig. 5; and the radius of each concentric circle is called window size in LSA. Fig. 5(a) shows that the initial interval between any two adjacent concentric circles is 1 unit (pixel), which is determined by the original resolution of the grid file. The increment of the calculation window can be set as 1 grid, that is the way in existing software when LSI is performed (see Fig. 5(a)). Nevertheless, it is too expensive to deal with big data since it needs higher computation cost. In BTLSM, the increment of calculation window can be determined as any natural numbers, which makes it possible to choose a suitable increment of calculation windows according to the initial resolution and the required precision. Fig. 5

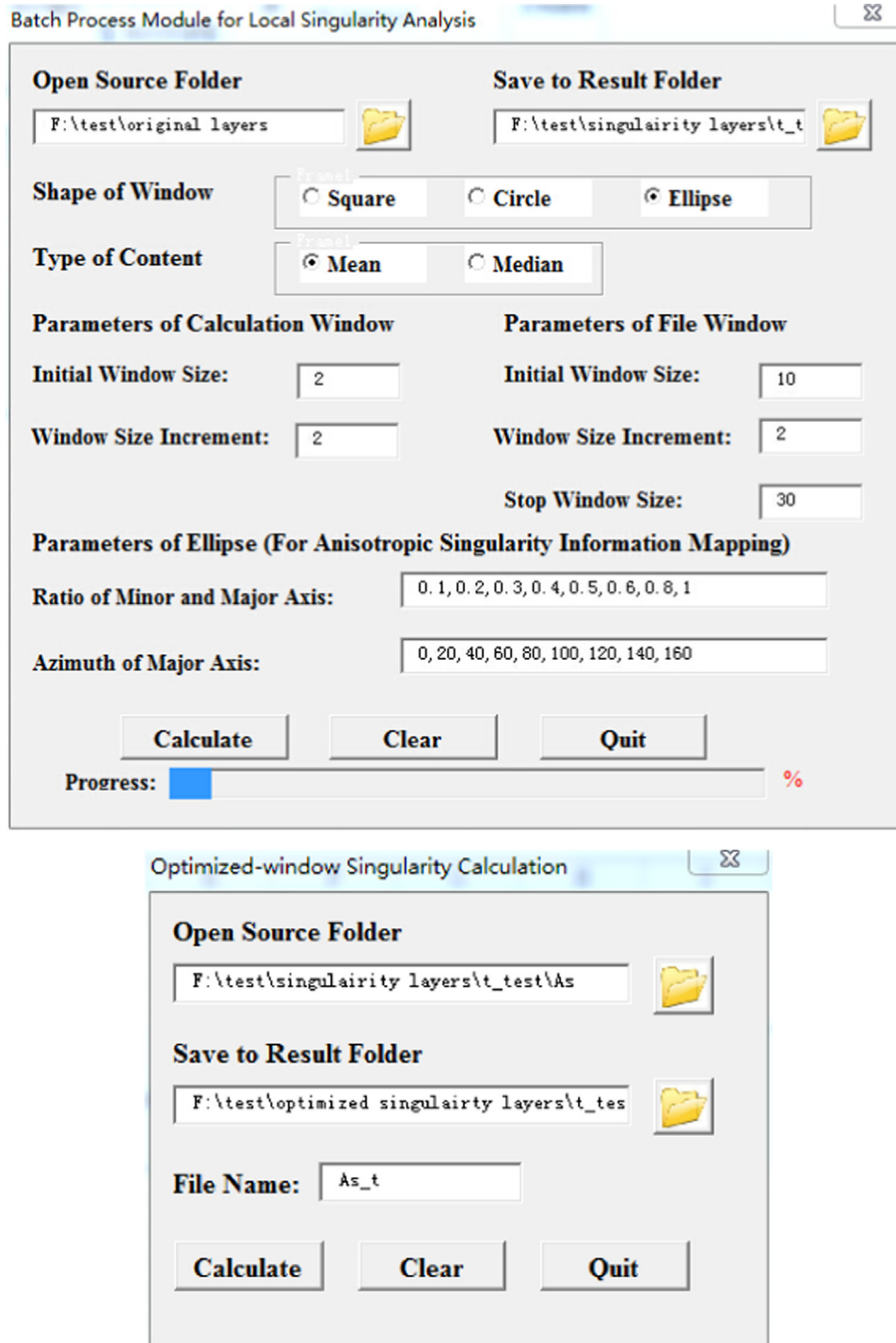


Fig. 4. User interfaces.

(b) shows the distribution of calculation windows (colored in yellow) when the increment is 2 grid, and in this condition the average content within the 1st, 3rd, 5th, 7th, 9th, 11th, 13th, 15th and 17th circles will be calculated respectively. Theoretically LSI layer could be obtained as long as there are more than 2 levels of calculation windows, because regression models could be established with 3 or more local window sizes which corresponds to different average contents. But sometimes we do not want to get LSI layer at each calculation window since it will result in too many files and cost lots of time and storage space. We can choose parts of the calculation windows as file windows, and Fig. 5 (c) provides a way. In Fig. 5(c), the window size of file window is

grown from 5 units to 17 units with an interval of 4 units, which means only LSI maps with maximum window size of 5, 9, 13 and 17 will be obtained. When the window size of file window is 5, the log values of the average contents within the 1st, 3rd, 5th circles, and the log values of corresponding window size allow fitting a straight line in rectangular coordinate system via the least squares method. Then LSI for the maximum window size of 5 can be obtained, and the LSI maps for window size of file window as 9, 13 and 17 can be obtained similarly. It is noted that the average value within each calculation window is calculated only once, although the results are used for the calculation of local singularity indices for different file windows.

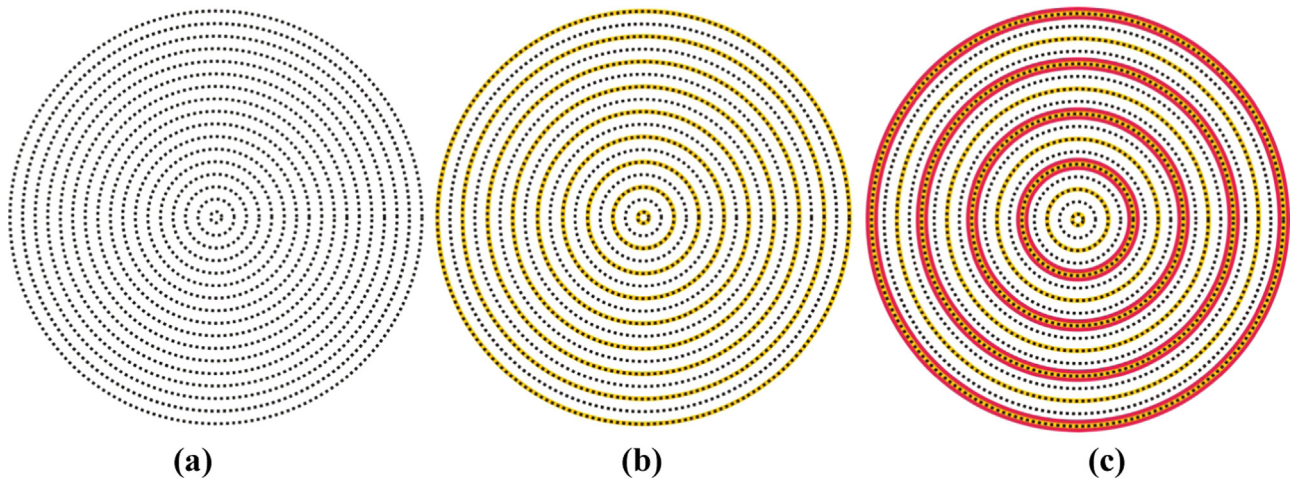


Fig. 5. Multiple-window for (a) initial windows, which reflect the original pixel size; (b) calculation windows, which reflect the expansion of present window at the speed of double original pixel size; and (c) file windows, which reflect that the LSI for certain LSI files would be saved. (For interpretation of the references to color in this figure, the reader is referred to the web version of this article.)

3.2.3. Local window shape

Three kinds of local window are provided here: i.e., square, circular, and elliptical. Square window procedures are similar to those for circular windows as introduced in preceding section, because both are isotropic windows. Nevertheless, the elliptical window is used to describe anisotropy, which can express more information, not only size but also compression and directivity. In the applications of this paper, window size is measured by means of the length of semi-major axis for the elliptical local window.

3.2.4. Content calculation methods within a local window

A common practice to express the content for a local window is using the mean value. However, the mean value can be affected by outliers, and it sometimes is better to use the median instead of the mean value. Therefore, both mean and median options are provided.

3.2.5. Anisotropy parameter design

When a square or circle is used to specify the local window, the only parameters that can be changed are concerned with the window size including initial window size, growing window size increases, and the maximum half-window size. However, there will be more parameters to be set when an elliptical window is used to describe the anisotropy of spatial distribution. In a two-dimensional coordinate system, when the location is given, three parameters being the length of the semi-major axis (i.e., the window size, as introduced in last session), azimuth, and ratio of the lengths of semi-minor and semi-major axes can be used to uniquely determine an ellipse. These three parameters are changeable and can be defined all at once.

3.2.6. Optimizing the local singularity index

Different kinds of singularity patterns can be obtained through different local window settings. For an elliptical window, different singularity patterns can be measured by varying not only the size but also the semi-major axis azimuth and the length ratio between the semi-minor and semi-major axes. So far all these applications are based on global criteria and the LSI maps are obtained based on the same local window parameters, and we can choose the best one from these maps according to their spatial correlation with the deposit layer. In fact, the optimized anisotropy parameters are changed everywhere. When a series of LSI maps are obtained using different local window parameters, statistical test parameters are also calculated, including goodness of fit (R^2) and

probability of t test. Thus it is possible to obtain an relatively optimized LSI value at each location according to R^2 or the confidence limit of t test; and the corresponding optimization parameters can also be recorded as layers, i.e. the maximum range, the azimuth of the semi-major axis, and the length ratio between the semi-minor and semi-major axis.

3.3. Key function

Build-in Excel functions have benefited our design a lot, among which *Linest* is the core function for calculation and optimization of LSI. The input of *Linest* consists of two vectors representing the logarithmically transformed window sizes and the average contents in the corresponding local window, and the output of *Linest* is a 5×2 array (see Table 1).

4. Case studies

The test data in this paper were taken from Cheng (2008)'s case study. The study area ($\approx 7780 \text{ km}^2$) is located in western Meguma Terrain of Nova Scotia, Canada. The lithological units in the study area are mainly Cambro-Ordovician low-middle grade metamorphosed sedimentary rocks and Devonian granitoid intrusions (Sangster 1990; Ryan and Ramsay 1997); the former are mainly NE–SW striking lower sand-dominated flysch Goldenville Formation and upper shaly flysch Halifax Formation, folded during Devonian granitoid intrusion emplacement (Kontak et al. 1998). The South Mountain Batholith (SMB), which is a complex of multi-phase granites, occurs mostly in the northern and southern parts of the study area (see Fig. 9). Significant Au (aurum), W (wolfram) and Sn (stannum) mineralization and mineral deposits have been

Table 1
Output of *Linest* function*.

	Column 1	Column 2
Row 1	$a1$	b
Row 2	$S(a1)$	$S(b)$
Row 3	R^2	$S(y)$
Row 4	t	d_f
Row 5	SSR	SSE

* Extracted from help text of Excel (with a slight change): $a1$ is the opposite of LSI, $S(a1)$ is standard error of LSI, R^2 is coefficient of determination, $t = a1/S(a1)$ is the observed value for t -test with $n-2$ degrees of freedom.

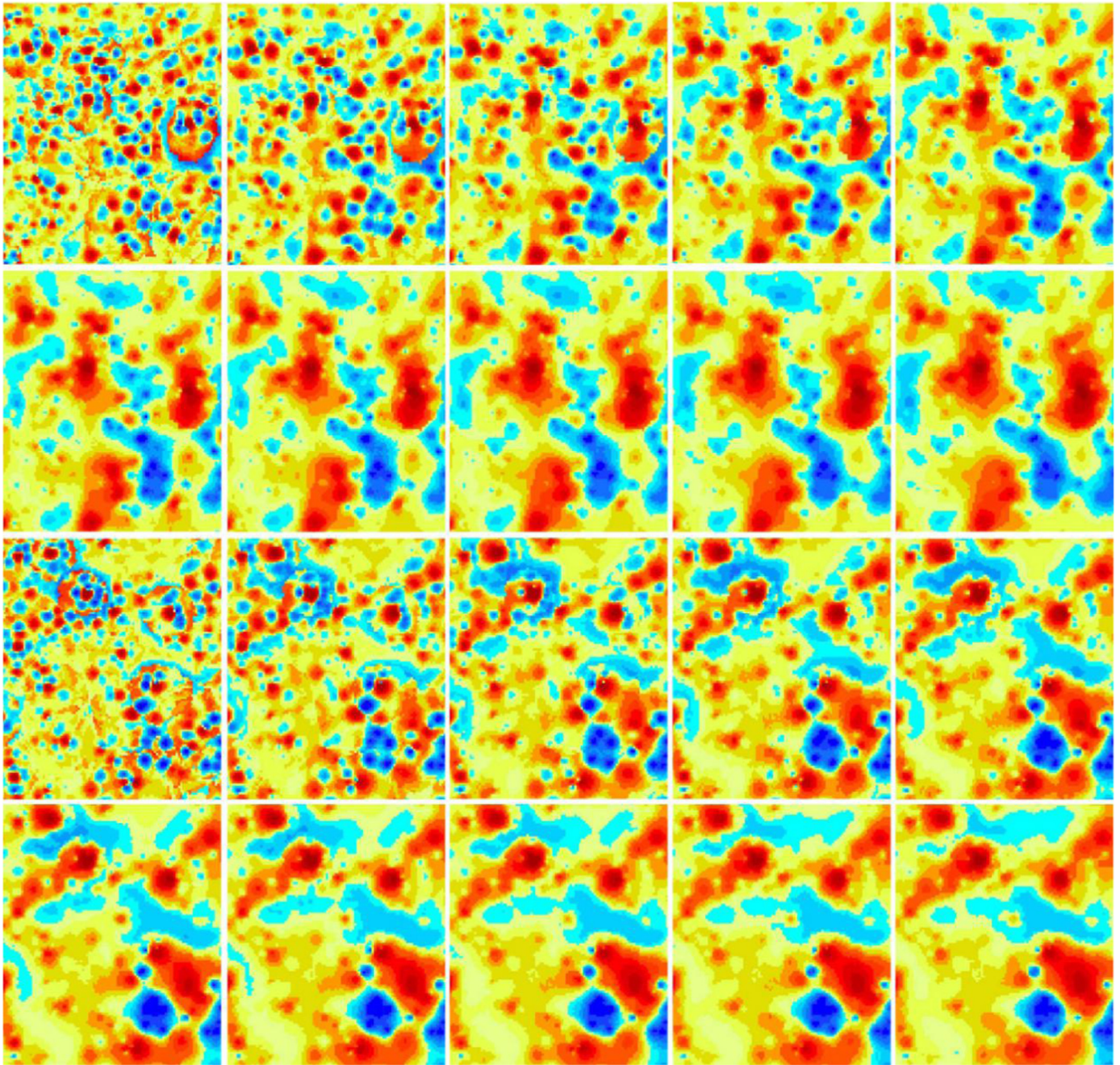


Fig. 6. Print screens of Local singularity index maps for square window. (For interpretation of the references to color in this figure, the reader is referred to the web version of this article.)

found in this area, including 20 Au deposits. With respect to geochemical exploration, there are 671 lake-sediment geochemical samples with sampling density as about 1 sample per 5 km². Former research has shown that both As (Arsenic) and Au concentration values have significant spatial relationship with the occurrences of Au deposits (Xu and Cheng, 2001). Therefore, all tests in this work are done on the relationship between Au deposits and these two elements, which are represented in the form of 500 m × 500 m grid layers.

4.1. Local singularity maps for square window

Firstly, the grid layers of elements As and Au were transformed into ASCII files. Secondly, input and output files were designated. Thirdly, the window shape and the content type were set as square

and mean respectively. Finally, the initial window size and the increasing window size for singularity calculation were set at 1 and 2; and the initial window size, the increasing window size and the stop window size for singularity files were set at 5, 4 and 41 respectively. As is discussed in Section 1, the traditional approach for LSI is to determine a set of local window parameters according to experience for the whole study area, e.g., 13 km is considered a good scale to extract geochemical anomaly in this study area. Nevertheless, it is common that a universally suitable local window may not exist in the whole study area, and that is why BTLSIM is developed in this research. In the new module, a discrete interval (i.e., from 5 to 41 as is shown above) is used instead of an isolated point (i.e., 13 according to experience), which can well combine prior knowledge and statistical quantitative laws. Different LSI maps of As and Au were obtained reflecting local anomalies at different spatial scales (see Fig. 6).

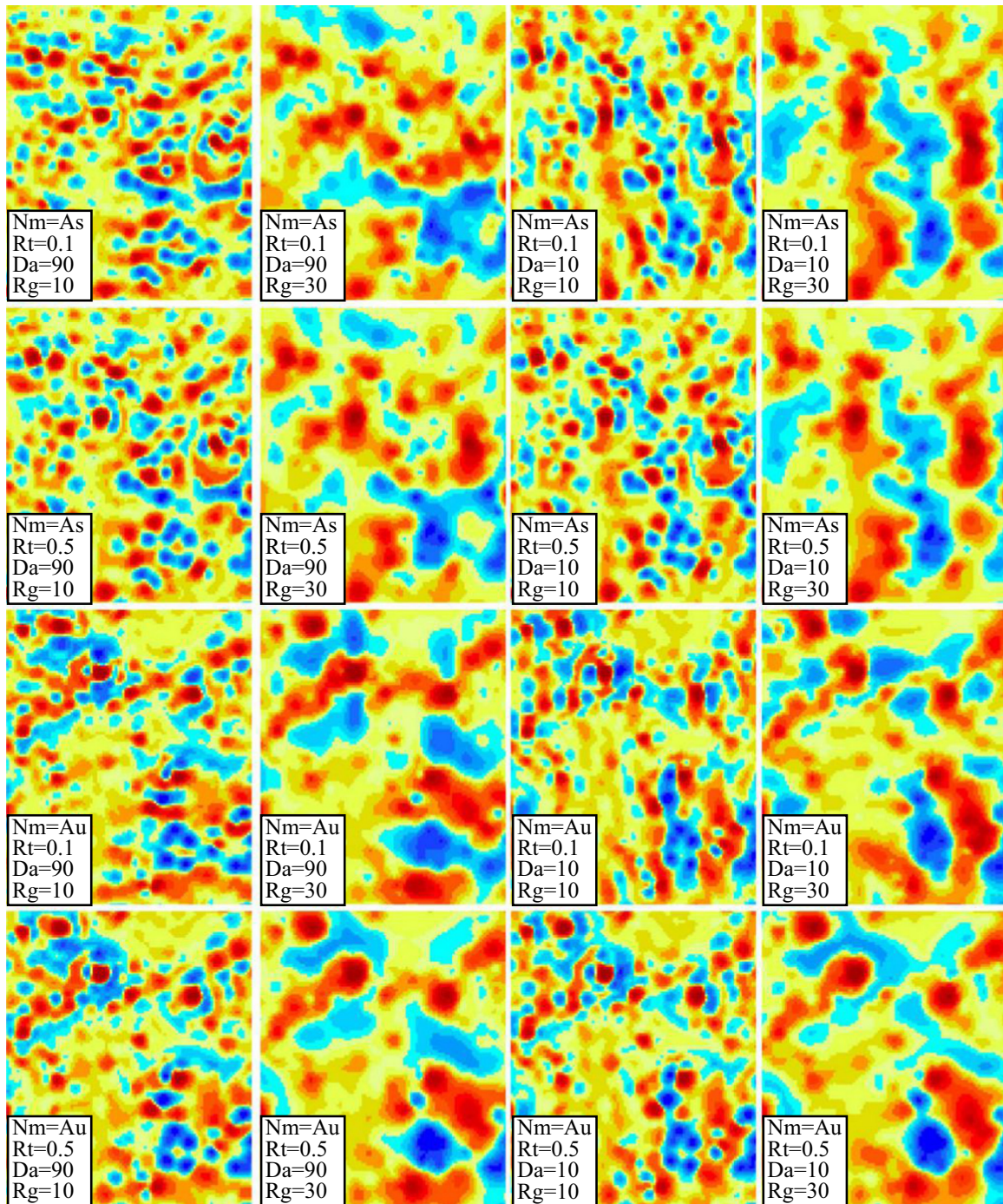


Fig. 7. Print screens of local singularity index maps with elliptical window.

Pictures in the first two rows and the last two rows are print screens of different window-size local singularity index maps for elements As and Au, respectively. From top to bottom, and from left to right, the maximum values of window size are 5, 9, 13, 17, 21, 25, 19, 33, 37, and 41 respectively. The hot colors (from red to orange according to the severity) represent high singularities while the cool colors (from blue to yellow according to the severity) represent low singularities. These pictures reflect changes of singularity form. On the one hand, the smaller the maximum window size is set, the more detailed the singularity becomes, but more noise is included; on the other hand, the larger the maximum window size is set, the more regular the singularity shapes become, but small size singularities may be filtered out.

4.2. Local singularity maps for elliptical window

The first step again was to transform the grid layers into text files and to designate the input and output folders. The type of local window used here was elliptical and content within local window was taken as mean value. More parameters have to be determined when an elliptical window is used to capture anomaly information due to anisotropy. The basis of determining parameters for an elliptical window is similar to Section 4.1, except that there are more parameters and we should also define discretization schemes for the azimuth angle and the compression for an ellipse. Here initial window size was set as 2 instead of 1 based on our understanding that the range of 3×3 could weaken the

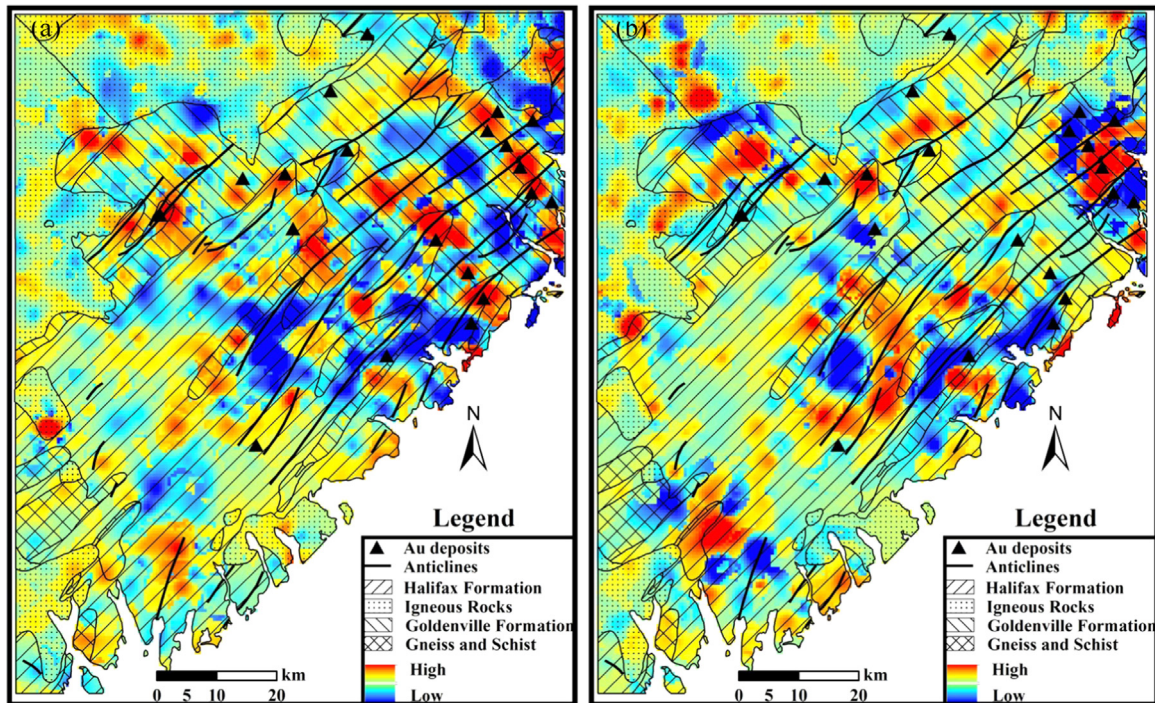


Fig. 8. Optimized local singularity mapping for (a) As and (b) Au.

effect of outliers and improve the precision of regression curve equation; increasing window size for singularity calculation were also set as 2, because increasing the increment of increasing window size can reduce the amount of computation and improve the operation efficiency. Initial window size, increasing window size and stop window size of file were set as 10, 2 and 30 respectively. That is because 13 km is considered as an empirical value with the scale of 1:200,000 and we choose a smaller value (10 km) for conservative estimation, and 30 km is considered as the maximum range for geological anomaly scope, and our set can guarantee obtain optimized LSI from 10 to 30. Besides, variogram, which is the basic tool of geostatistics can also be used to determine the ranges for local window size. Minimum and maximum value of the length ratio between the semi-minor and semi-major axes of the elliptical window were set at 0.1 and 1, with increments of 0.1 for equal dividing. Minimum and maximum value of the azimuth angle of the ellipse semi-major axis were set at 0° and 160° , with increments of 20° , which is also for equal dividing. Because the direction of the semi-major axis in an elliptical window is perpendicular to the trend of original element contents, we have used the singularity direction instead of the semi-major axis direction. Screenshots of parts of all 1980 LSI maps are shown in Fig. 6. It can be seen that the singularity patterns are affected greatly by the azimuth and the length ratio between semi-minor and semi-major axes of the elliptical window. The resulting singularity patterns also are related to the window size, as they were for the square and the circular windows. An elliptical window makes it possible for users to extract certain forms of mineral anomaly; e.g., if singularity information for a certain direction is to be extracted, the corresponding azimuth parameter should be set for this direction (Fig. 7).

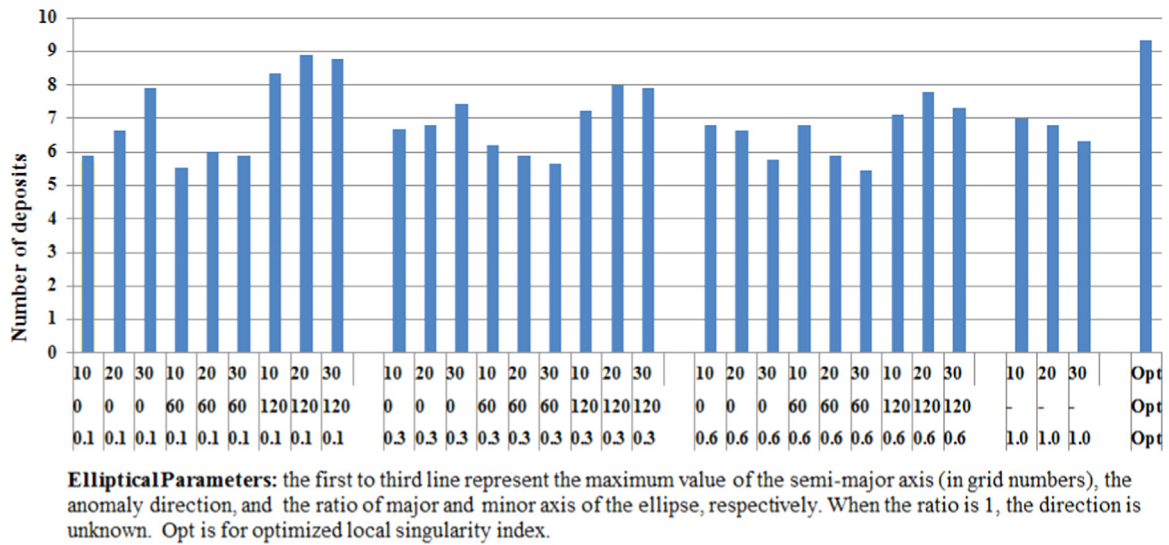
Pictures in the first two rows and the last two rows are print screens of different window-size local singularity index maps for As and Au, respectively. Element name and elliptical window parameters are shown in the left corner of each picture: Nm (name) is short for element name; Rt (ratio) represents the ratio of major and minor axis of the ellipse; Da (direction angle) means azimuth angle of the ellipse's semi-major axis, in degrees; Rg

(range) represents maximum value of the semi-major axis, which represents the range of the singularity, in grid numbers.

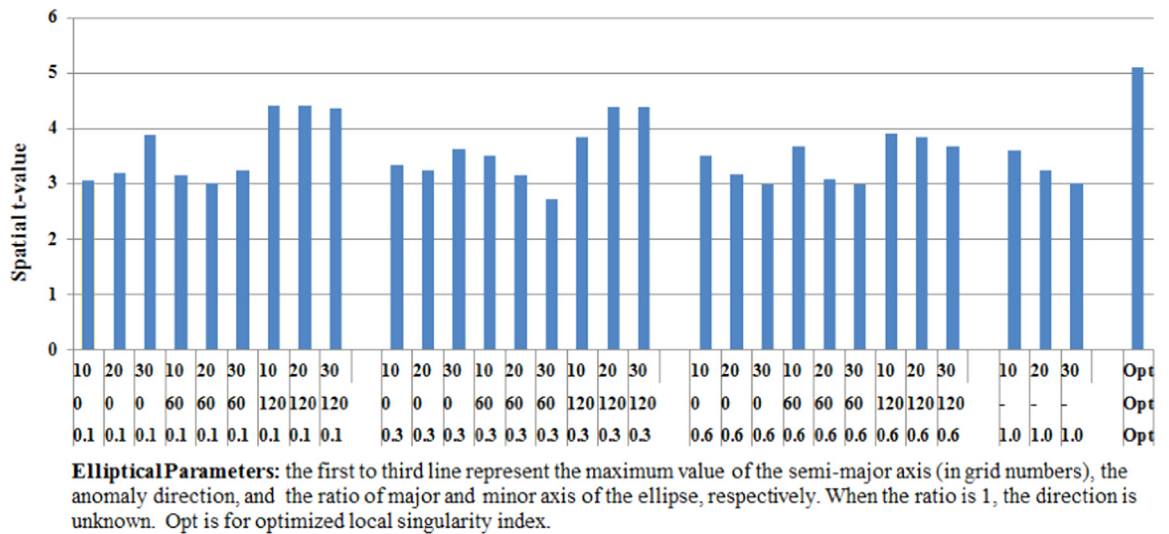
4.3. Optimized local singularity mapping

Based on a series of local singularity maps obtained under different window parameters, optimized LSI maps were obtained according to *t*-statistics (see Fig. 8a and b. As is described in Table 1, LSI has 1 degree of freedom when *t* test is performed since $n=2$). It can be seen from Fig. 8 that both overall trend and local details are captured, with the maxima showing good spatial correlation with the Au deposits. It could also be seen from Fig. 8 that although the study area is totally controlled by northeastern structure, beaded anomalies stretching northwestwardly shows much closer relationship with the known Au deposits, which is in good agreement with previous studies. In order to compare optimized LSI and the single window parameter maps, results of further tests for the element As are shown in Fig. 9, for which 30 maps were selected from 902 single-parameter based LSI maps.

Fig. 9(a) shows the known deposit numbers located at the top 10% area according to the LSI maps for the element As based on different elliptical windows. From the left to the right, four clusters of pillars which represent different ratios of minor and major axes suggest self-similarity in the first three clusters, and this suggests that the spatial distribution of the anisotropy parameters does have certain rules to follow. The fourth cluster is incomplete and only the parameter of window size works. This is because when the ratio between minor and major axes is 1, an elliptical window reduces into a circular window. Among all three elliptical parameters, direction provides most discrimination, and the singularity maps with azimuth of 120° (which is close to the optimum direction in Fig. 10(a) show higher scores. When the optimum direction is determined, it can be seen that a smaller length ratio between minor and major axes can leads to better performance. Regulation of the lengths of major axes is difficult because it is hard to determine a single optimal window size for the whole study area. Thus it is necessary to find a best local window for every location in the study area. The optimized LSI layer shows



(a)



(b)

Fig. 9. Performance of optimized LSI map and single local window parameter maps according to (a) known deposit numbers located at the top 10% area, and (b) the maximum *t*-value.

higher score than any LSI layers based on single local window parameters. This further indicates that the optimizing method is not only necessary, but also useful for information extraction in mineral exploration. In order to further verify the significant for the above observation, spatial *t* test developed by Agterberg and Cheng, 2002 is also performed here. In the spatial *t* test, a bigger *t* value means stronger spatial relationship between two layers. The *t*-value in Fig. 9(b) shows similar regularities and the optimized LSI has the largest *t*-value. In Fig. 9(b), *t*-values on each map are obtained by firstly reclassifying the grids into 20 classes based on equal-area method, and then determining the largest *t*-values using GeoDAS software.

It should be noticed that all LSI maps were obtained without deposit training. Under this condition, any improvement in best area score or *t*-value will lead to better prediction, without the problem of over-fitting.

In addition, maps which reflect the anisotropy of As and Au were also obtained. These include the spatial distribution of window size (variable range), major axis azimuth of elliptical window, and ratio between minor and major axes of the ellipse (see

Fig. 10a–f). Such maps are of significance in detecting the structure of spatial anisotropy for geochemical elements.

Pictures in the first and second rows are spatial anisotropy parameters maps for As and Au respectively. Pictures in the first column are for the mapping of azimuth angles, in degrees, which reflect direction of the anisotropy; the second column maps show the range of semi-major axis, in meters, which reflect the size of singularity; the last column shows maps for the ratio of the length between the minor and major axes of the elliptical window, and reflects the intensity of anisotropy.

In this study area, there exists dominating anisotropic trends; e.g., the approximately 160° direction controlling almost the whole study area is stable whereas other directions are located in corridors between areas for this main direction. Anisotropy parameters such as preferred direction can become a powerful factor to improve mineral prediction.

Taking the element As for example, a histogram representing the grid counting for different directions is shown in Fig. 11. It can be seen that the SSE–NNW direction with azimuth of about 160° constitutes the majority of the total grid numbers. An amplified map representing anisotropy parameters for the black rectangle in

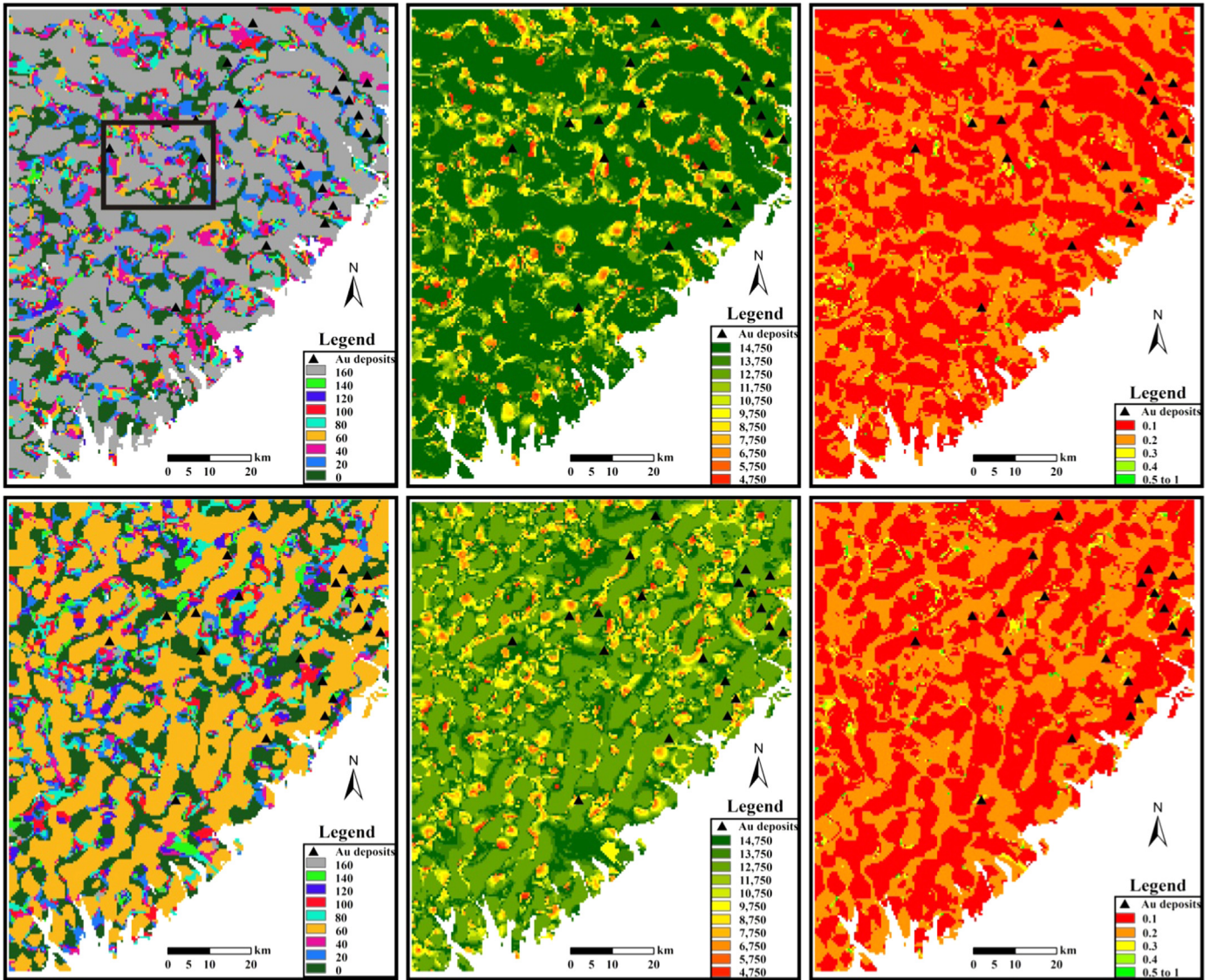


Fig. 10. Spatial anisotropy parameters mapping.

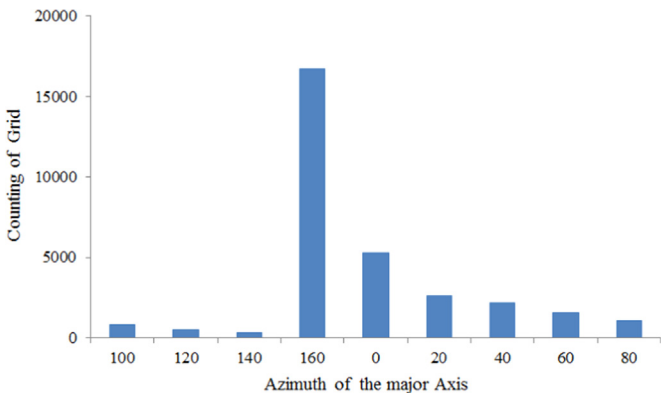


Fig. 11. Grid counting for different fitted directions.

Fig. 10(a) is shown in Fig. 12, for which only the SSE–NNW direction is retained. It can be seen from Fig. 12 that spatial anisotropy in the SSE–NNW direction is dominant.

Red points represent deposits. For the purpose of clarity, the lengths of semi-minor and semi-major axes of the ellipse were reduced 40 times.

4.4. Discussion

In this case, Optimized LSI not only shows better predicted results than any single-window LSI layer, but also provides layers for anisotropic parameters, which have the potential to display more information on geology and mineralization. Since LSA is a non-training model and performed without known Au occurrences, any improvement on prediction performance is objective and credible, and there is need to worry about over-fitting.

5. Conclusions

In this paper, Excel software, together with the development method VBA, was used to build the BTLSIM software module. Several objectives were achieved: (1) BTLSIM reduces manual operations and improves efficiency; (2) it offers more parameter selections for LSA allowing the use of different types of local windows including anisotropic windows to explore different forms of singularities, and both mean value and median value can be used to represent the average content for the local window; and (3) it presents a relatively self-adaptive local singularity determination algorithm which can result in an optimized LSI map,

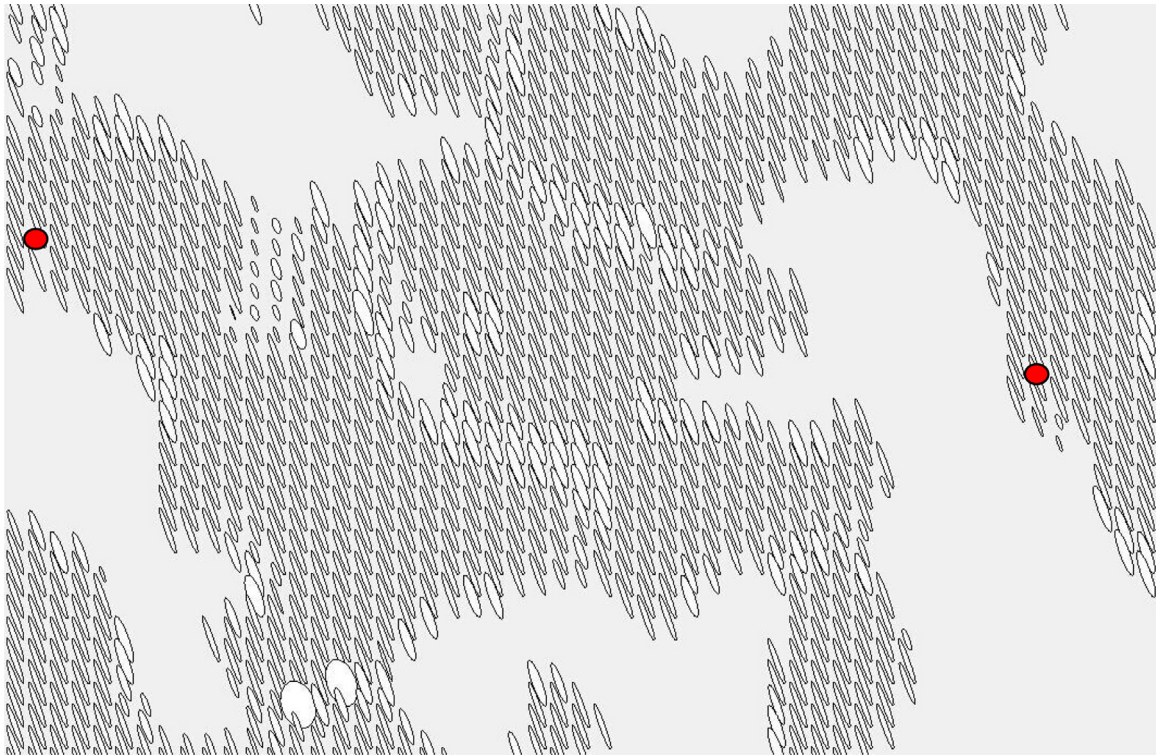


Fig. 12. Best ellipses for the calculation of local singularity index in space according to t -test.

providing three kinds of parameter layers for variable range, direction, and compressibility of anisotropy in space, respectively.

The case study has shown that optimized LSI maps have better spatial relationship with Au deposits than single-window based ones, which means optimized LSI is an improvement of LSI. And anisotropy layers obtained along with the optimized LSI layer can benefit further research on the spatial structure of geoscience variables.

Another advantage of BTL SIM is that the widespread availability of Excel will facilitate its usage since no extra software installation steps are needed, and it has been made sure that BTL SIM could be used in different Excel versions (from Excel 2007 to Excel 2016).

The limitations of this research include that we are not so clear about the meaning of the anisotropic patterns other than the domain direction.

Acknowledgments

This research is financially supported by the Program of Integrated Prediction of Mineral Resources in Covered Areas (No. 1212011085468) awarded by China Geological Survey.

Appendix A. Supplementary material

Supplementary data associated with this article can be found in the online version at <http://dx.doi.org/10.1016/j.cageo.2015.12.012>.

References

- Agterberg, F.P., Cheng, Q., 2002. Conditional independence test for weights-of-evidence modeling. *Nat. Resour. Res.* 11 (4), 249–255.
- Chen, G., Cheng, Q., Liu, T., Yang, Y., 2013. Mapping local singularities using magnetic data to investigate the volcanic rocks of the Qikou depression, Dagang oilfield, eastern China. *Nonlinear Process Geophys.*, 20.
- Chen, G., Cheng, Q., Zuo, R., Liu, T., Xi, Y., 2015. Identifying gravity anomalies caused by granitic intrusions in Nanling mineral district, China: a multifractal perspective. *Geophys. Prospect.* 63, 256–270.
- Chen, Z., 2007. Multifractal theory based local singularity analysis method and its application in spatial information extraction for mineral exploration (Dissertation). China University of Geosciences, Wuhan.
- Chen, Z., Cheng, Q., 2007a. Generalized local singularity analysis and its application. *J. China Univ. Geosci.* 18 (Special issue), 348–350.
- Chen, Z., Cheng, Q., Chen, J., 2014. Iterative approach to local singularity analysis and software implementation based on raster data. *J. Geol.* 38 (4), 613–622.
- Chen, Z., Cheng, Q., Xie, S., Chen, J., 2007b. A novel iterative approach for mapping local singularities from geochemical data. *Nonlinear Process Geophys.* 14, 317–324.
- Cheng, Q., 1996. *Multifractal Modelling and Spatial Analysis with Gis: Gold Potential Estimation in the Mitchell-sulphurets Area, Northwestern British Columbia*. University of Ottawa, Canada.
- Cheng, Q., 1997. Fractal/multifractal modeling and spatial analysis. Keynote Lecture in Proceedings of the International Mathematical Geology Association Conference. Vol. 1, pp. 57–72.
- Cheng, Q., 1999a. Spatial and scaling modelling for geochemical anomaly separation. *J. Geochem. Explor.* 65, 175–194.
- Cheng, Q., 1999b. Multifractal interpolation. In: Proceedings of the Annual Conference of the International Association for Mathematical Geology. Trondheim, Norway, pp. 6–11.
- Cheng, Q., 2004. Quantifying the generalized self-similarity of spatial patterns for mineral resource assessment. *Earth Sci.* 29, 733–743.
- Cheng, Q., 2005. A new model for incorporating spatial association and singularity in interpolation of exploratory data. *Geostatistics Banff 2004*, 1017–1025, Springer.
- Cheng, Q., 2006a. Singularity-generalized self-similarity-fractal spectrum (3S) models. *Earth Sci. – J. China Univ. Geosci.* 31, 337–348.
- Cheng, Q., 2006b. GIS-based multifractal anomaly analysis for prediction of mineralization and mineral deposits. In: Harris, J. (Ed.), *GIS for the Earth sciences*. Geological Association of Canada, Tri-Co Group, Ottawa, pp. 285–296.
- Cheng, Q., 2007. Mapping singularities with stream sediment geochemical data for prediction of undiscovered mineral deposits in Gejiu, Yunnan Province, China. *Ore Geol. Rev.* 32, 314–324.
- Cheng, Q., 2008. Non-Linear Theory and Power-Law Models for Information Integration and Mineral Resources Quantitative Assessments. *Math. Geosci.* 40, 503–532.
- Cheng, Q., Agterberg, F., Ballantyne, S., 1994. The separation of geochemical anomalies from background by fractal methods. *J. Geochem. Explor.* 51, 109–130.
- Cheng, Q., Agterberg, F., Bonham-Carter, G., 1996. A spatial analysis method for geochemical anomaly separation. *J. Geochem. Explor.* 56, 183–195.
- Govett, G.J.S., Goodfellow, W.D., Chapman, R.P., Chork, C.Y., 1975. *Exploration*

- geochemistry—distribution of elements and recognition of anomalies. *J. Int. Assoc. Math. Geol.* 7 (5–6), 415–446.
- Harris, J.R., Wilkinson, L., Grunsky, E., Heather, K., Ayer, J., 1999. Techniques for analysis and visualization of lithochemical data with applications to the Swayze greenstone belt, Ontario. *J. Geochem. Explor.* 67 (1), 301–334.
- Harris, J.R., Wilkinson, L., Grunsky, E.C., 2000. Effective use and interpretation of lithochemical data in regional mineral exploration programs: application of Geographic Information Systems (GIS) technology. *Ore Geol. Rev.* 16 (3), 107–143.
- Hu, S., Cheng, Q., Wang, L., Xu, D., 2012. Modeling land price distribution using multifractal IDW interpolation and fractal filtering method. *Landsch. Urban Plan.* 110, 25–35.
- Kontak, D.J., Horne, R.J., Sandeman, H., Archibald, D., Lee, J.K., 1998. 40Ar/39Ar dating of ribbon-textured veins and wall-rock material from Meguma lode gold deposits, Nova Scotia: implications for timing and duration of vein formation in slate-belt hosted vein gold deposits. *Can. J. Earth Sci.* 35 (7), 746–761.
- Li, C., Ma, T., Shi, J., 2003. Application of a fractal method relating concentrations and distances for separation of geochemical anomalies from background. *J. Geochem. Explor.* 77 (2), 167–175.
- Liu, Y., Cheng, Q., Xia, Q., Wang, X., 2013a. Application of singularity analysis for mineral potential identification using geochemical data—A case study: Nanling W–Sn–Mo polymetallic metallogenic belt, South China. *J. Geochem. Explor.* 134, 61–72.
- Liu, Y., Xia, Q., Cheng, Q., Wang, X., 2013b. Application of singularity theory and logistic regression model for tungsten polymetallic potential mapping. *Non-linear Process. Geophys.* 20 (4), 445–453.
- Mandelbrot, B.B., 1975. Stochastic models for the Earth's relief, the shape and the fractal dimension of the coastlines, and the number-area rule for islands. *Proc. Natl. Acad. Sci.* 72, 3825–3828.
- Miesch, A.T., 1981. Estimation of the geochemical threshold and its statistical significance. *J. Geochem. Explor.* 16 (1), 49–76.
- Neta, T., Cheng, Q., Bello, R.L., Hu, B., 2010. Upscaling reflectance information of lichens and mosses using a singularity index: a case study of the Hudson Bay Lowlands, Canada. *Biogeosci. Discuss.* 7 (3), 3551–3578.
- Ryan, R.J., Ramsay, W.R.H., 1997. Preliminary comparison of gold field in the Meguma Terrain, Nova Scotia, and Victoria, Australia. In: Macdonald, D.R., Mills, K. A. (Eds.), *Mines and Mineral Branch. Report of Activities 1996; 1997*, pp. 157–162.
- Sangster, A.L., 1990. Metallogeny of the Meguma Terrain, Nova Scotia. In: Sangster, A.L. (Ed.), *Mineral Deposit Studies In Nova Scotia 90-8*. Geological Survey of Canada, Canada, pp. 115–152. Paper.
- Sinclair, A.J., 1974. Selection of threshold values in geochemical data using probability graphs. *J. Geochem. Explor.* 3 (2), 129–149.
- Stanley, C.R., Sinclair, A.J., 1989. Comparison of probability plots and the gap statistic in the selection of thresholds for exploration geochemistry data. *J. Geochem. Explor.* 32 (1), 355–357.
- Wang, W., Zhao, J., Cheng, Q., 2013. Application of singularity index mapping technique to gravity/magnetic data analysis in southeastern Yunnan mineral district, China. *J. Appl. Geophys.* 92, 39–49.
- Wang, W., Zhao, J., Cheng, Q., Liu, J., 2012. Tectonic-geochemical exploration modeling for characterizing geo-anomalies in southeastern Yunnan district, China. *J. Geochem. Explor.* 122, 71–80.
- Xie, S., Cheng, Q., Ke, X., Bao, Z., Wang, C., Quan, H., 2008. Identification of geochemical anomaly by multifractal analysis. *J. China Univ. Geosci.* 19, 334–342.
- Xu, Y., Cheng, Q., 2001. A fractal filtering technique for processing regional geochemical maps for mineral exploration. *Geochemistry: Explor. Environ. Anal.* 1 (2), 147–156.
- Zhang, D., Cheng, Q., Agterberg, F., 2014. *An Application of Equal-Area-Growing Window for Calculating Local Singularity for Mapping Granites in Inner Mongolia Mathematics of Planet Earth*. Springer, Germany, pp. 73–77.
- Zuo, R., Cheng, Q., 2008. Mapping singularities—a technique to identify potential Cu mineral deposits using sediment geochemical data, an example for Tibet, west China. *Miner. Mag.* 72, 531–534.
- Zuo, R., Cheng, Q., Agterberg, F.P., Xia, Q., 2009. Application of singularity mapping technique to identify local anomalies using stream sediment geochemical data, a case study from Gangdese, Tibet, western China. *J. Geochem. Explor.* 101 (3), 225–235.
- Zuo, R., Wang, J., Chen, G., Yang, M., 2015. Identification of weak anomalies: a multifractal perspective. *J. Geochem. Explor.* 148, 12–24.
- Zuo, R., Xia, Q., Zhang, D., 2013. A comparison study of the C–A and S–A models with singularity analysis to identify geochemical anomalies in covered areas. *Appl. Geochem.* 33, 165–172.